

Analysis of High L:D Freewing Solar Platform

by Galen J. Suppes, PhD, PE

March, 16, 2021 (DRAFT)

Abstract

The burgeoning aerial drone industry has the opportunity to overcome paradigms that have limited performance of contemporary manned aircraft. In particular, both flat low-drag-profile aircraft and flat plate airfoil technology can achieve higher lift to drag ratios (L:D) for "Low Profile Drones". Analysis of a solar plane using solar cells on towed platforms identifies an approach to achieve faster, more efficient, and smaller scale aircraft capable of 24/7 sustained solar flight.

Estimates of maximum attainable lift were calculated for a towed platform. The results were used to: a) compare to benchmark aircraft performances, b) identify conditions for optimizing efficiency, and c) project performance of aerial solar platform trains. Low Profile Drones are estimated to achieve overall L:D > 40:1 and enable solar powered aircraft for a range of previously unattainable applications.

Introduction

A solar aircraft ("SP-Drone") designed for 24/7 cruising uses a rectangular freewing to achieve ultra-high lift-to-drag ratios (See Figure 1) for cruising in the stratosphere. One application of 24/7 solar aircraft is for local communication systems, including expected product introductions by AeroVironment and Boeing. AeroVironment claims one aircraft in a 125 mile diameter flight path can provide service equivalent to 1,800 cell towers.

SP-Drone targets higher-velocity, more-robust, and more-versatile performance in this burgeoning market. This enables more applications and smaller-scale less-expensive vehicles. Three novel design features of SP-Drone include:

1. Solar power collection can be incrementally added by adding towed platforms in a train-like configuration resembling a towed banner.
2. Towed platforms connect through front hinge joints that allow the platforms to passively adjust to low air angles of attack with very high lift-to-drag (L:D) ratios.
3. A flat profile, relatively low lateral span, and train streamlining allow for ultra-low form drag which translate to ultra-high overall L:D ratios and high speed capabilities.
4. Hinge joint flexibility and stacking of the towed platforms for takeoff and landing provide for robust designs.

These features combine to enable higher loads, faster velocities, feasibility at smaller scales, and strategic combinations of these capabilities.

This design brings forth fundamental questions on the limits of performance of the flat plate airfoil, which is the model approximation of the towed platform. Questions emerge on the ultimate performance (i.e. L:D) of the towed platforms relative to conventional wings. These questions are particularly relevant because of the ability of the towed platform, in principle, to both exceed performances of contemporary alternatives and to approach the performance of the simple model approximation.

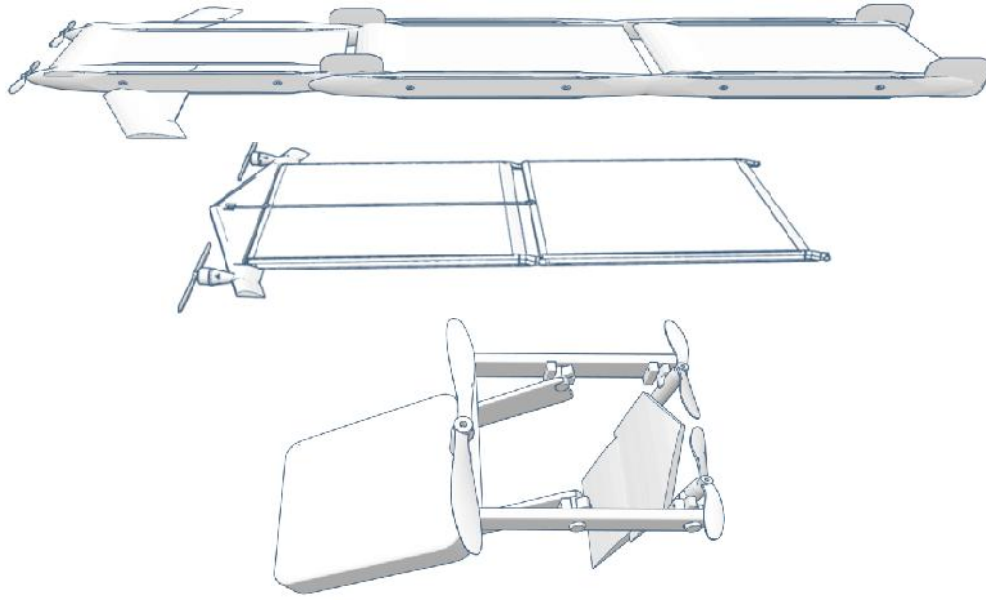


Figure 1. Transformer and SP-Drone configurations with one towed platform.

This paper uses an energy balance on air interacting with the flat plate airfoil surface to estimate maximum lift potential and performance trends based on maximizing favorable velocity-pressure conversions. An energy balance and mass balance around constant volume cubical control volumes provides the maximum lift that can be generated by a surface. It is equivalent to assuming perfect laminar flow. Those results are compared to benchmark performances and used to interpret the performance potential.

Theoretical Foundation

Figure 2 illustrates coordinates for the subsequent energy balance is performed. The control volumes of analysis are a series of cubical volumes perpendicular to the surface along the z-axis having a width dx and length dy .

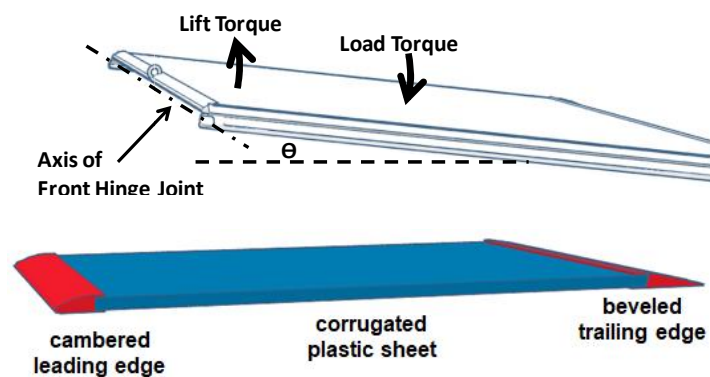


Figure 2. Side view of flat plate part of flat plate airfoil illustrating variables and axis of analysis.

For a series of cubic volumes along the z-axis at steady state and distant from side or edge effects, the flows are equal and opposite for opposite sides and for the leading versus trailing edges. Since side and edge conditions cancel, analysis simplifies to a one-dimensional analysis along the z axis.

Air enters the lower surface at $\mathbf{v} \sin(\theta)$ where θ is air's angle of attack and \mathbf{v} is relative velocity. Air exits the lower surface at negligible kinetic energy as an expansion process equal in mass flow rate to the air entering the lower surface. The following applies:

- Air enter with a kinetic energy of $0.5 \dot{m} \mathbf{v}^2$, and
- air exits at the same mass flow as the entering air but as a slight expansion of the cube volume where the kinetic energy of the exiting air is negligible, and
- air exits with a slight increase in temperature and pressure representative of isentropic, adiabatic compression where polytropic equations apply, and
- if C_p is used for the energy calculation the enthalpy of the exiting air accounts for both the pressure and temperature component of air's internal energy.

Upper surfaces have opposite flows that of lower surfaces with kinetic energy leaving and air of slightly higher temperature entering.

The value of \mathbf{v} next to the surface is zero with a maximum value is equal to the speed of the flat plate airfoil relative to ambient air. These set boundary conditions for analysis along the z axis.

The energy balance of the system is defined by equation 1.

$$\text{Total Energy} = \text{Internal Energy} + \text{Kinetic Energy} + \text{Potential Energy} + \text{Work} + \text{Heat Transfer} \quad (1)$$

Interpretation of kinetic energy change in air versus work or shaft work and steady state.

$$\text{Constant} = \text{Internal Energy} + \text{Kinetic Energy} \quad (2)$$

For the control volume:

$$E_{Total} = 0.5 \dot{m} \frac{dv^2}{dz} + \dot{m} \frac{dH}{dz} \quad (3)$$

Where analysis is for air.

$$0 = 0.5 \dot{m} \frac{dv^2}{dz} + \dot{m} \frac{dH}{dz} = 0.5 \dot{m} \frac{dv^2}{dz} + \dot{m} \frac{C_p dT}{dz} \quad (4)$$

The mass flow rate to and from the control volume is $\theta \dot{m}$; it divides out of Equation 4.

For an integral analysis for ideal-gas air for velocity from $\mathbf{v} = \mathbf{v}_{max}$ to $\mathbf{v} = \mathbf{0}$ at the surface:

$$0.5 v_{max}^2 = -C_p \Delta T \quad (5)$$

Where $C_p = 1.0 \text{ kJ/kg/K}$ for air and $\gamma = C_p/C_v = 1.4$ as an approximation for ideal gas near 300 K. The energy of an ideal gas is independent of pressure and density; this is a natural fallout of an ideal gas having no molecule-molecule interaction (including no volume exclusion associated with collision). For an isentropic adiabotic process.

$$\left(\frac{T_2}{T_1}\right) = \left(\frac{P_2}{P_1}\right)^{(\gamma-1)/\gamma} \quad (6)$$

Air's angle of attack does not show up in these calculations (discussed later). Lift is calculated by the surface integral of the following equation:

$$Lift = \oint \frac{\Delta P dA}{\sin(\theta)} \quad (7)$$

The drag associated with the lift is:

$$Drag = \oint \frac{\Delta P dA}{\cos(\theta)} \quad (8)$$

For a flat surface θ is constant and the lift-to-drag ratio at low angles is equal to θ in radians (degrees * $\pi/180$), thus:

$$L:D = \frac{1}{\tan(\theta)} \quad \text{where} \quad \lim_{\theta \rightarrow 0} \left(\frac{1}{\tan(\theta)} \right) = \frac{1}{\theta} \quad (9)$$

These equations relate a change in pressure to a change in velocity due to the conservation of energy in a steady-state volume. Use of Equations 5 and 6 to calculate lift pressure compare to velocity-pressure conversion of the Bernoulli equation as follows:

$$0.5 \Delta(\rho v_{max}^2) = \Delta P \quad (10)$$

where ρ is the density of air.

Results

Equation Artifacts - The derivations identify that the pressure generated due to velocity is independent of the angle of attack, which may be counter-intuitive. However, the calculations assume a steady-state condition consistent with a very large surface having negligible side and edge effects. It is reasonable that for a large surface the pressure generated by a gas is independent of air's angle of attack.

Example Calculation -The following values are assumed in example calculations: $v = 100$ m/s (360 km/hr, 224 mph), $T_1 = 273$ K, $P_1 = 1E5$ kg /s²/m (~1 atm), $C_p = 1000$ kg m²/s²/kg/K (ideal gas air), $\gamma = C_p/C_v = 1.4$, $R = 287$ m²/s²/K, and $\rho = P/RT$ ($\rho_1 = P_1/RT_1 = 1.28$ kg/m³). For ideal gas isentropic/adiabatic, the specific kinetic energy is 5,000 m²/s², $T_2/T_1 = 278/273$, $P_2/P_1 = 1.0656$ with a ΔP on one plate surface of 0.0656 atm (0.964 lb/in²; 138.8 lb/ft²), or 278 lb/ft² for both sides of surface. For the Bernoulli equation, $\Delta P = 5,000 * 1.28$ m²kg / m³ s² or 0.064 atm or 135 lb / ft².

Table 1 summarizes the maximum lift loads of the ideal gas model as a function of velocity and air angle of attack. The load is proportional to the ambient pressure and is provided at: 1) 1.0 atm for takeoff/landing and 2) 0.1 for cruising in the lower stratosphere. In the upper atmosphere, ambient pressures are less than 0.01 atm.

Table 1. Estimated best lift loads accounting for upper and lower surface of plate. Lift in N/m² is 48 times lift in lb/ft².

| Lift (lb/ft ²) | Velocity (mph) | Velocity (kph) | Lift Load (lb/ft ²) | | | | | | | |
|-------------------------------|-------------------|----------------------|------------------------------------|-------|-------|-------|-------|-------|-------|-------|
| | | | 0.05 | 0.52 | 5.24 | 26.2 | 0.005 | 0.052 | 0.52 | 2.62 |
| 0 | 31.1 | 50 | 0.05 | 0.52 | 5.24 | 26.2 | 0.005 | 0.052 | 0.52 | 2.62 |
| 0 | 62.1 | 100 | 0.21 | 2.10 | 21.01 | 105 | 0.021 | 0.210 | 2.10 | 10.51 |
| 0 | 93.2 | 150 | 0.47 | 4.75 | 47.49 | 237 | 0.047 | 0.47 | 4.7 | 23.7 |
| 0 | 124.2 | 200 | 0.85 | 8.50 | 84.95 | 425 | 0.085 | 0.85 | 8.5 | 42.5 |
| 0 | 186.3 | 300 | 1.95 | 19 | 195 | 973 | 0.195 | 1.95 | 19.5 | 97.3 |
| 0 | 310.6 | 500 | 5.71 | 57 | 571 | 2857 | 0.57 | 5.71 | 57.1 | 286 |
| 0 | 434.8 | 700 | 12.16 | 122 | 1216 | 6081 | 1.22 | 12.16 | 121.6 | 608 |
| 0 | 559.0 | 900 | 22.39 | 224 | 2239 | 11193 | 2.24 | 22.39 | 223.9 | 1119 |
| | | P ₁ (atm) | 1.0 | 1.0 | 1.0 | 1.0 | 0.1 | 0.1 | 0.1 | 0.1 |
| | | θ' (°) | 0.01 | 0.1 | 1 | 5 | 0.01 | 0.1 | 1 | 5 |
| | | L:D | 5730 | 573 | 57 | 11 | 5730 | 573 | 57 | 11 |
| | | cos(θ) | 1.000 | 1.000 | 1.000 | 0.996 | 1.000 | 1.000 | 1.000 | 0.996 |

Isentropic Assumption - It is well-accepted that air's kinetic energy transforms to a pressure changes in the process of generating lift. For this process in an aircraft, there are several possible sources of irreversibility, including the irreversibility of the energy transformations and resistance to air flow. Aircraft with smooth surfaces report L:D ratios typically in excess of 10:1 and up to 70:1. These high values substantiate that for smooth surfaces in streamlined designs, the transformation from velocity to pressure and back is highly efficiency. This substantiates that the isentropic assumption has value as a point of reference that can be approached.

Drag and irreversibilities occur and are increasingly impacting at L:D projections greater than 100:1. Values larger tha 100:1 are highly dependent on specifics of streamlining and surface smoothness. For a flat plate airfoil, specifying θ also defines the L:D as summarized in Table 1. Values of L:D greater than 200 cannot be realistically approached due to shear drag becoming significant.

Zero Velocity at Surface - The assumption of velocity proceeding from a maximum value to zero is founded in the no-slip condition at the surface, which by definition is a zero relative velocity at the surface. Laiminar flow dictates a continuous and smooth change in velocity from the surface to the maximum velocity at a point distant from the surface.

Velocity to pressure calculations are often calculated using Bernoulli flight theories, ban arbitrary velocity is selected. That arbitrary velocity typically, conveniently results in a pressure change that validates the approach.

The present analysis is an estimate of the maximum lift and surface loading.

Two-Surface Assumption - The equation derivation and example calculations are for the underside of an airfoil with air approaching at a maximum velocity distant from the surface and reducing to zero under the no-slip condition at the surface. An interpretation on the upperside of the surface assumes that the air of zero velocity is pulled by the no-slip condition to achieve a maximum velocity on the upperside of the surface. The result is a negative pressure change on the upperside approximately equal and opposite the pressure change on the underside.

Impact of Surrounding Pressure - For both the ideal gas and Bernouli Equation approaches, the lift load is proportional to ambient pressure.

Power versus Speed - A vehicle at constant weight (load) requires the same lift at all velocities during steady-state flight. At all velocities for a flat plate airfoil this translates to: a) the same specific lift load (ΔP), b) the same drag, and c) the same drag. Energy requirements are proportional to the **Drag X Distance**. The power requirement is proportional to **Drag X Distance X v**. This translates to power being proportional to velocity.

Since the **Lift Load** is proportional to ambient pressure, the steady-state flight power requirements are proportional to P_1 (Equation 6, ambient pressure). This translates to a 10X increase in power to maintain flight at 48,000 ft altitude versus sea level (neglecting changes in shear drag). At 78,000 ft, power requirements are 100X that at sea level. In equation form:

$$SSPower \propto 101,300 (1 - 0.00002256 h)^{5.256} \quad (11)$$

where **SSpower** is steady-state thrust power requirement at altitude h in meters.
(see https://www.engineeringtoolbox.com/air-altitude-pressure-d_462.html)

Discussion

Interpretation of Results - Despite substantially different assumptions, the loading (lb/ft²) is similar for the two approaches. Example wing loading range from 0.2-4.1 for birds, 3.7-10.4 for gliders, 14.3-26 for prop aircraft, and 58-168 lb/ft² for jet engines. These values correlate well with velocity of flight where increased flight velocities enable increased loads. Loads attained by the aircraft are about half the maximum loads of Table 1.

Typical passenger jet takeoff velocities are 150 to 180 mph with wing loadings of 100 to 150 lb/ft². For takeoff (1 atm), Table 1 identifies that velocities in excess of about 100 mph attain needed loadings at an aircraft pitch of about 5°. For cruising at 0.2 atm, a speed of 400 mph and an angle of about 3° translate to an L:D of about 20:1; which is qualitatively correct by interpolation.

For an infinitely large flat plate, the interpretation of total conversion of kinetic energy to/from pressure for lift is reasonable.

Leading and trailing edge effects can be overcome with the same features used in contemporary wing/airfoil designs. The contemporary airfoils' canopy feature is designed to provide for rapid formation toward desired pressure profiles in the longitudinal direction.

Fences on sides flat plate airfoils can reduce the cancelling flow of lower-surface higher pressure air to the upper surface. Data is needed to identify the tradeoff between fence height and increased lift, but it is anticipated that fence heights of 4X the thickness of the front airfoil canopy feature.

Airfoil Comparison - The perfectly flat plate surface allows all pressure to manifest as lift at a maximum L:D, and because of this, a flat plate airfoil is able to achieve L:D in excess of 100:1. By comparison, the best wing airfoils have maximum L:D only slightly over 70:1. The Eta glider a wide wingspan aircraft that reports an L:D of 70:1. A towed flat plate airfoil with front hinge joint passively adjusts pitch so that lift load is equal and opposite an evenly distributed airfoil load. Solar cells distributed on a flat plate airfoil with a front hinge joint is a practical application of this technology.

The following is a comparison of PROS and CONS of structural wings versus flat plate airfoils:

PROS of Contemporary Airfoils:

- Greater thickness allows internal structures of ribs, stringers, and spurs for lateral transfer of load (load does not have to be evenly distributed).
- Provides a range of pitch orientations velocities where lift is only a moderate function of velocity and pitch (lift on flat plate airfoil is proportional to velocity and pitch at low air angles of attack).
- Design provides good pitch and yaw stability when properly combined with a fuselage.

PROS of Flat Plate Airfoils:

- Capable of greater L:D than contemporary airfoils.
- Passive stability overcomes pitch and yaw stability problems when towed with a front hinge joint (towing has passive yaw stability, a front hinge joint allows flat plate to pivot until lift matches load).
- Good match with solar plane application where solar cells can be arranged as an evenly distributed load.
- A single sheet can provide lift on both the upper and lower surfaces resulting in less than half the weight of a wing for providing lift on upper and lower surfaces.

In this comparison, contemporary wings and flat plate airfoils, each, have applications of distinct performance advantages. Under these conditions, a combination is often able to achieve the best of both capabilities.

Figure 3 illustrates a freewing flat plate airfoil connected to an aircraft with wings, propulsors, ailerons, and landing gear. Features of the large flat plate area that could cause pitch instability are overcome by the passively stable pitch adjustment. Unlike the towed platform of Figure 1, the platform of Figure 3 is substantially surrounded by an aircraft having wings. The Figure 3 configuration is particularly useful for takeoff and landing. The flat plate of Figure 3 could be multiple stacked platforms that are extended during flight to form a train. Payload compartments could be integrated into either the freewing flat plate or the winged aircraft as optimal to application-specific designs.

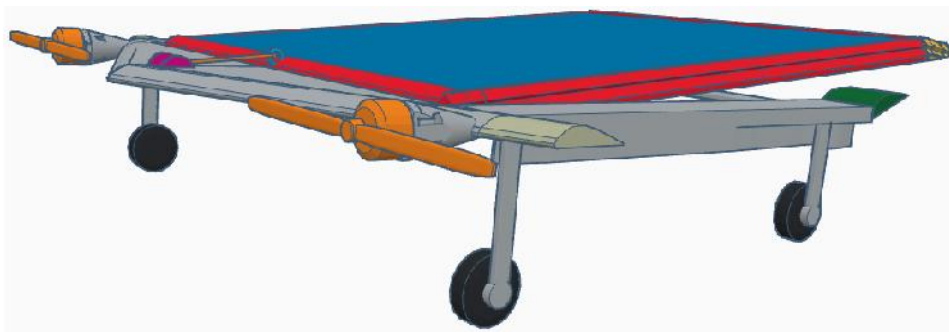


Figure 3. Pitch-stable front aircraft design.

Applications - Figure 4 illustrates an SP-Drone train configuration. For the solar-powered aircraft application, the towed platforms are towed with collecting solar energy while the lead aircraft is tasked with the payload as well as collecting solar energy. For communications, the payload and energy storage can be relatively light. It is possible for the payload to include a range of options including stored energy, chemical production and storage, parcel/freight transit, passenger transit, pod/passenger transfer service, military arsenal, radar, and traditional satellite functions like imagery.



Figure 4. Pitch-stable front aircraft design.

The train's L:D is the total lift over the total drag. Equation 12 summarizes a calculation of L:D for a train:

$$L:D_{Overall} = \frac{\frac{W_F + N}{W_T}}{\frac{W_F}{(L:D)_F W_T} + \frac{N}{(L:D)_T}} \quad (12)$$

where W is weight, F designates front vehicle, T designated towed platform, and N is the number of towed platforms.

In the limit of large N , the overall L:D approaches the towed platform L:D. The modular nature of adding additional towed platforms of similar design has additional advantages related to manufacturing and maintenance.

Solar cells are available at less than 0.16 lb/ft² (see spectrolab.com) and corrugated plastic is available at less than 0.15 lb/ft². The respective towed platform could achieve L:D greater than 100. At a load of 0.31 lb_f/ft² (14.88 N/m²) and 100 m/s; the drag is at a rate of 14.88 W/m². Energy collection is 135 mW/cm² or 1,350 W/m². As a result, at 100 m/s the power generation of the solar platform is about 100X the energy to sustain flight. Taking into account hours of sunlight and efficiency in storage, this translates to about 30X the energy needed for 24/7 flight.

With this high-end performance, it is possible to attach panels behind a passenger aircraft for passenger service using renewable solar energy at velocities similar to jet aircraft. These aircraft could have L:D superior to today's best passenger aircraft, but that L:D is less an issue of renewable solar energy is used to power flight.

The lack of clouds, increased solar intensity, ability to orient the platform for morning/evening light, and ability to extend hours of daylight by travel against earth's rotation at night allow solar panels on SP-Drone to achieve up to about 3.5X the solar productivity on Earth's surface. This can take solar energy from being marginally economically viable to being highly profitable; and that enables use of solar energy to produce hydrogen and chemicals on stratospheric platforms. Unlike facilities on Earth's surface, flying facilities have neither greenfield costs nor maintenance associated with dust/vegetation. Large volume production of hydrogen for energy and ammonia for fertilizer (or energy) can realized new and improved production economies.

L:D Dependence on Velocity for Towed Platforms – For a towed flat plate airfoil, the ΔP term of Equation 1 applies to both drag and lift, and it is set by the load (does not change with velocity). An increase in velocity decreases θ ; the total wetted surface area (A_{WSA}) is constant; and Equation 13 relates A_{FCS} to A_{WSA} . Equation 13 can be used in the Equation 8 integral for drag per Equation 14.

$$A_{FCS} = 0.5 \theta A_{WSA}; \quad D = \theta A_{WSA} \Delta P \quad (13), (14)$$

Equation 14 identifies that D decreases as θ decreases, and so, D decreases as v increases. This may seem to defy common sense, but it is actually straight forward logic. Since ΔP is constant and increasing velocity decreases A_{FCS} , the drag of the plate surfaces must decrease with increasing velocity.

Figure 2 shows a platform side cross-section where a large sheet connected to a cambered leading edge and a beveled trailing edge. For prototyping, corrugated plastic is commonly used with RC aircraft and provides a light-weight structure with some rigidity. That leading edge does not have the same drag dynamics as the large midsection sheet, but that leading edge is also relatively small in frontal cross section area for a large sheet. The actual drag profile of towed platform is highly dependent on the size/shape of the cambered leading edge and its size relative to the sheet. As an estimate, the drag of the entire platform is considered to be constant with increasing velocity (versus decreasing for a perfect flat plate). The result is Equation 9, which should be a reasonable correlation for a range of useful combinations of sheets and cambered leading edges.

$$Power \propto v \quad (\text{for a towed platform}) \quad (15)$$

Conclusions

An energy balance on aerodynamic compression and expansion of air flow around a flat plate airfoil predicts reasonable upper end limits of pressure forces on a surface as a function of velocity and ambient air pressure. The simplified analysis possible for a flat plate airfoil allows the calculation of corresponding upper end limits of lift and L:D.

A more-in-depth technical discussion is provided as an Appendix A (pages 14-15) to preserve the flow of presentation of the innovations. Summary of key points of the theory, calculations, and heuristics of Appendix A are as follows:

- The towed platform is a key feature of SP-Drone and some fuselages of Transformer Drone; it is approximated as a flat plate airfoil as illustrated by Figure 2.
- Very high L:D (>100:1, see Figure 10) are a “geometric mandate”, where the challenge is to maintain stable flight at $0.2^\circ < \theta < 1.0^\circ$.
- Whereas power needs are proportional to v^3 for typical wing airfoils, a better estimate for the flat plate airfoil is power proportional to velocity (v), which makes high velocity flight more feasible/preferred for towed platforms.
- A practical flat plate airfoil (see Figure 2) has a cambered leading edge that rapidly develops desired pressure profiles in the direction of air flow; that leading edge is a disproportionate source of drag, but it is critical for high performance.